Palaeogeography, Palaeoclimatology, Palaeoecology 651 (2024) 112392

Contents lists available at ScienceDirect

Palaeogeography, Palaeoclimatology, Palaeoecology

journal homepage: www.elsevier.com/locate/palaeo

RAD-seq data for *Engelhardia roxburghiana* provide insights into the palaeogeography of Hainan Island and its relationship to mainland China since the late Eocene

Pei-Han Huang [a,b,f], Tian-Rui Wang [b,c,f], Min Li [a,f], Zi-Jia Lu [b,e], Ren-Ping Su [a,f], Ou-Yan Fang [a,f], Lang Li [a], Shi-Shun Zhou [d], Yun-Hong Tan [d], Hong-Hu Meng [a,d,*], Yi-Gang Song [b,*], Jie Li [a,*]

[a] *Plant Phylogenetics and Conservation Group, Center for Integrative Conservation & Yunnan Key Laboratory for Conservation of Tropical Rainforests and Asian Elephants, Xishuangbanna Tropical Botanical Garden, Chinese Academy of Sciences, Mengla 666303, China*
[b] *Eastern China Conservation Centre for Wild Endangered Plant Resources, Shanghai Chenshan Botanical Garden, Shanghai 201602, China*
[c] *Wuhan Botanical Garden, Chinese Academy of Sciences, Wuhan 430074, China*
[d] *Southeast Asia Biodiversity Research Institute, Chinese Academy of Sciences, Nay Pyi Taw 05282, Myanmar*
[e] *College of Life Sciences, Shanghai Normal University, 100 Guilin Rd., Shanghai 200234, China*
[f] *University of Chinese Academy of Sciences, Beijing 100049, China*

ARTICLE INFO

Editor: H. Falcon-Lang

Keywords:
Hainan Island
Geology history
Evolutionary trajectory
Climate change
RAD-seq
Engelhardia roxburghiana

ABSTRACT

Hainan Island in southern China is situated within the Indo-Burma biodiversity hotspot, and has attracted the attention of evolutionary biologists, geologists, and biogeographers. However, the palaeogeography of Hainan Island and its relationship with mainland China remains contested. In this paper, we report RAD-seq data for *Engelhardia roxburghiana* populations from Hainan Island and adjacent mainland areas to identify genetic diversity, structure, divergence time, and demographic dynamics over geologic time. Findings were assessed using climate model data to constrain suitable distribution areas. Results indicate that *E. roxburghiana* dispersed from the Chinese mainland to Hainan Island via a hypothetical land bridge during the late Eocene so that the drift of Hainan Island was impossible. We cast doubt on the hypothesis that Hainan Island was connected to Vietnam and Guangxi at this time. We emphasize that higher genetic diversity in the Yunnan-Guizhou Plateau and Chiang-nan regions is the result of mixed populations or the existence of refugia, and lower genetic diversity in the Indochina Peninsula is due to a historical bottleneck. From the late Eocene to Oligocene, the arid belt that dominated East Asia retreated, facilitating the expansion of *E. roxburghiana* from the Indochina Peninsula to southern China. The main diversification of *E. roxburghiana* occurred in the Miocene following the strengthening precipitation within the East Asian Summer Monsoon. Climatic oscillations during the Quaternary led to the contraction of *E. roxburghiana* in the Indochina Peninsula, with expansion after Last Glacial Period (LGP; 119 to 11.7 ka). Southern China has served as a refugium and continues to do so in the future. In summary, our study elucidates the evolutionary trajectory of *E. roxburghiana* through large-scale sampling, providing insights into the palaeogeography of Hainan Island and itsbiogeographic relationships with adjacent mainlands.

1. Introduction

Islands serve as crucial "natural laboratories" for exploring evolutionary processes, dynamics, and distribution patterns. These unique environments have consistently captured the attention of naturalists such as Charles R. Darwin and Alfred R. Wallace since the 19th century (Darwin, 1859; Wallace, 1860; Helmus et al., 2014). Their ideal settings make islands suitable for in-depth studies in ecology (Gillespie, 2015; Graham et al., 2017), evolution (Emerson, 2008; Losos and Ricklefs, 2009; Lamichhaney et al., 2015; Shaw and Gillespie, 2016), biogeography (Chen et al., 2023; Liu et al., 2023; Whittaker et al., 2017; Hirschfeld et al., 2023; Zhang et al., 2023), and biodiversity conservation (Nogué et al., 2017; Bosch et al., 2023).

Various types of islands exist on Earth, each with distinct origins leading to diverse biotas and unique characteristics (Cox et al., 2016). Continental-shelf islands (e.g., Hainan Island), which may have once

* Corresponding authors at: Southeast Asia Biodiversity Research Institute, Chinese Academy of Sciences, Nay Pyi Taw 05282, Myanmar.
E-mail addresses: menghonghu@xtbg.ac.cn (H.-H. Meng), ygsong@cemps.ac.cn (Y.-G. Song), jieli@xtbg.ac.cn (J. Li).

https://doi.org/10.1016/j.palaeo.2024.112392
Received 28 March 2024; Received in revised form 19 July 2024; Accepted 19 July 2024
Available online 24 July 2024

been connected to the mainland by land bridges, allowing for the development of endemic species while isolated (Matthews and Triantis, 2017). Unlike oceanic islands (e.g., Hawaii and the Galapagos), which emerge from oceanic crust without terrestrial connection to the mainland, continental-shelf islands may experience periodic separation and reconnection to the mainland due to fluctuations in sea levels (Lambeck et al., 2002; Whittaker and Fernández-Palacios, 2007). Therefore, investigating the relationship between continental-shelf islands and their adjacent mainland offers valuable insights into biotic evolutionary processes on both islands and adjacent mainlands.

Hainan Island is the largest continental-shelf island in the northern part of the South China Sea (SCS; Fig. S1) and lies within the Indo-Burma biodiversity hotspot (Myers et al., 2000). Situated in the southern part of China, east of Vietnam across the Beibuwan, it is separated from the Leizhou Peninsula of mainland China by the shallow and narrow Qiongzhou Strait (Fig. S1; Zhao et al., 2007; Shi et al., 2002). The unique tropical flora of Hainan Island has long fascinated ecologists, biologists, and geologists, prompting investigations into the origin of the island's flora and the distribution patterns of its biota. Historically, Hainan Island was considered part of Cathaysia (most parts of southern China, especially the Chiang-nan ranges), which was connected to the Leizhou Peninsula of the mainland (Chen, 1956; Hou, 1992). However, rising sea levels during the mid-Holocene flooded low-lying parts of the Leizhou Peninsula, leading to the formation of the Qiongzhou Strait (Lin and Zong, 1987; Zhao et al., 2007). In recent years, some researchers have hypothesized that Hainan Island was once connected to Guangxi and Vietnam and then moved and rotated to its present location; they relied on the ancient vicariance to explain the origin of island's biota (Mo and Shi, 1987; Zhu, 2016, 2017, 2020; Liang, 2013, 2018). However, based on available geological evidence, the idea of plate-tectonic drift cannot be substantiated (Ali, 2018). Previous studies in this area were primarily based on comparing floristic compositions or conducting small-scale sampling analyses to obtain geological evidence of Hainan Island and neighboring landmasses (Zhu, 2016; Liang et al., 2018; Huang et al., 2019). To better explore the biogeographic patterns of both Hainan Island and its neighboring landmasses, large-scale sampling in Hainan Island and along the neighboring mainlands, should be combined with advanced molecular biological evidence (Meng and Song, 2023).

Engelhardia roxburghiana Wall., a wind-pollinated tropical and subtropical evergreen tree of the walnut family (Juglandaceae), exhibits a wide distribution from subtropical China to Indonesia (Meng et al., 2022b; Zhang et al., 2020). Notably, its extensive range, spanning Hainan Island and neighboring regions as well as both subtropical and tropical zones, suggesting its adaptability and dispersal mechanisms in diverse climatic and geological conditions. *E. roxburghiana* is characterized by even-pinnate leaves, dark-brown or black twigs, and leaflets typically arranged in 3–5 pairs, most featuring a short acuminate apex and seven (5–13) pairs of secondary leaflet veins (Lu et al., 1999; Meng et al., 2022a, 2022b; Zhang et al., 2020). Fruit fossils of *Engelhardieae* provide a rich Cenozoic record in the Northern Hemisphere (Manchester, 1987, Manchester et al., 1994; Jin, 2009; Meng et al., 2015; Hermsen and Gandolfo, 2016), including an Eocene occurrence in Hainan Island (Jin et al., 2009). Additionally, fossil records of numerous taxa from the Eocene and Oligocene found on Hainan Island indicated that it was part of the Pan Gulf of Tonkin palaeoflora (Huang et al., 2022). The distribution pattern of *E. roxburghiana*, along with the fossil records, provides a valuable framework for investigating the biogeographic history of this taxon in Hainan Island and the adjacent mainlands, as well as investigate the evolutionary trajectories of the lineage in these regions.

In this study, we used restriction site-associated DNA sequencing (RAD-seq) to explore genetic diversity, structure, and population demographic history. In addition, we tested hypotheses regarding the spatiotemporal history of Hainan Island and the adjacent landmasses, focusing on the biological consequences of palaeogeographical events. Thus, our objectives were to: (1) elucidate the genetic diversity and structure of *E. roxburghiana* at the molecular level; (2) confirm biogeographic patterns between Hainan Island and the adjacent mainlands using *E. roxburghiana*; and (3) illuminate the evolutionary trajectory of *E. roxburghiana* from the Indochina Peninsula to southern China.

2. Materials and methods

2.1. Sampling

A total of 242 individuals of *E. roxburghiana* were collected from 50 locations in Hainan Island and its neighboring landmasses (Fig. S1 and Table S1). Fresh leaves of these trees were dried using silica gel, with a minimum distance of 50 m maintained between sampled individuals within each population. The sampling sites were sourced from the Chinese Virtual Herbarium (CVH; https://www.cvh.ac.cn), the Global Biodiversity Information Facility (GBIF; https://www. gbif.org), and the Flora of China (FOC; Lu et al., 1999). Additionally, eight individuals of *Rhoiptelea chiliantha* from one population were collected as the outgroup, chosen based on their phylogenetic positions within Juglandaceae (Zhang et al., 2020; Meng et al., 2022a, 2022b). Notably, there is no *E. roxburghiana* population in the Leizhou Peninsula due to the missing of records of Herbarium, and we did not discover this species there during fieldwork.

2.2. Library protocols

DNA of *E. roxburghiana* was extracted using a modified cetyltrimethyl ammonium bromide (CTAB) method (Doyle and Doyle, 1987). Subsequently, all genomic DNA samples were sent to BGI (Shenzhen, Guangdong, China) for library construction and sequencing. Genomic DNA was digested using the restriction enzyme *Eco*RI, followed by ligation of the P1 adapter. Pooled fragments were randomly sheared, and fragments 300–500 bp in length were selected. Another adapter (P2) was ligated to retrieve the DNA fragments, which were then selectively amplified by PCR. Qualification and quantification of the libraries were performed using the Agilent 2100 Bioanalyzer and quantitative PCR. Raw data consisting of 150 bp paired-end reads were generated using the Illumina HiSeq XTen sequencing platform.

2.3. Data processing

To retain high-quality reads, the raw data were evaluated and quality-controlled using SOAPnuke v1.05 (Chen et al., 2017), focusing on parameters such as GC content and Q20 rate. Clean reads were processed into single nucleotide polymorphisms (SNPs) using Stacks v2.41 (Catchen et al., 2013). Initially, the process_radtags module in Stacks was used to filter the overall quality of the reads, demultiplex them, and trim the reads to 120 bp. Given that the reference genome of the species itself tends to be prioritized in RAD-seq studies (Huang et al., 2024), the reference genome of *E. roxburghiana* was obtained from (https://cmb.bnu.edu.cn/juglans/; Ding et al., 2023) and indexed using BWA v0.7.17 (Li and Durbin, 2009). Subsequently, BWA-MEM algorithm (Li, 2013) was used to map sequence reads from 242 individuals to the reference genome. SAMTOOLS v1.10 (Li et al., 2009) was used to sort the aligned reads and assess the mapping rate. Then, we used the gstacks module, incorporating paired-end reads aligned to the reference genome to create loci and sort them. Relative filters were applied in populations module. A filtering parameter of $-r = 0.8$ was set where $\geq$80% of individuals in a population were required to process a locus. Removing sites showing heterozygosity >0.7 to reduce the potential occurrence of paralogs, then filtered the dataset for minor allele frequencies (MAF) > 0.1, and only the first SNP per locus was retained. Additional filtering was conducted using VCFtools v0.1.16 (Danecek et al., 2011) and Plink v1.07 (Purcell et al., 2007). We used VCFtools to filter sites based on a minimum average read depth of 5 and missing data proportion < 0.1. Plink was used to exclude sites with linkage

disequilibrium and to retain biallelic SNPs.

2.4. Population structure

Population genetic structure was evaluated by Bayesian clustering and principal component analysis (PCA). To estimate the number of genetic clusters, Bayesian clustering was performed using STRUCTURE v2.3.4 (Pritchard et al., 2000). The analysis was performed 10 times with K values ranging from 1 to 10, each run consisting of 10^6 Markov chain Monte Carlo (MCMC) generations. The optimal number of clusters (K) was determined using STRUCTURE HARVESTER (Earl and von-Holdt, 2012) with the Delta-K method (Evanno et al., 2005). PCA was calculated using Plink. The principal components (PCs) were extracted using the –pca parameter. To confirm the subsection structure of all 242 individuals, the first two PCs (PC1, PC2) were visualized in R v4.2.2 (Core Team, 2022) using the "FactoMineR" (Lê et al., 2008), "factoextra" (Kassambara and Mundt, 2020) and "ggplot2" (Wickham, 2016) packages.

2.5. Phylogeny and divergence time

Bayesian inference (BI) and maximum likelihood (ML) were performed to analyze the phylogeny of *E. roxburghiana* lineages, with *R. chiliantha* selected as the outgroup. IQ-tree v1.6.12 (Nguyen et al., 2015) was used to reconstruct the ML tree, in which the best-fit substitution model was automatically selected by the software. A BI tree with Markov chains was reconstructed using BEAST v2.6.0 (Bouckaert et al., 2014) for runs with a length of 2.5×10^8 generations, sampling every 10^4 generations. The initial 30% of the samples were discarded as burn-in. FigTree software v1.4.4 (http://tree.bio.ed.ac.uk/software/figtree/) was used to visualize the final phylogenetic tree.

According to the Bayesian MCMC algorithm, we used BEAST to estimate the divergence time. The GTR + G model was selected as the optimal alternative model using the Akaike information criterion (AIC) implemented in jModeltest v2.1.7 (Darriba et al., 2012). A lognormal relaxed clock model was used, and the Yule process was chosen as the tree prior. Based on the phylogeny of Juglandaceae, the BI tree was calibrated using three fossils. *Budvaricarpus serialis*, with an estimated range from 89.8 to 83.6 Ma (Heřmanová et al., 2011; Ding et al., 2023), was used to calibrate the stem age. *Alatonucula ignis*, which occurs in South America, is the most reliable and oldest known fruit fossil on record (Hermsen and Gandolfo, 2016). It has an $^{40}Ar/^{39}Ar$ age of 52.22 ± 0.22 Ma (Wilf, 2012; Barreda et al., 2020) and was used to calibrate the crown age. The Eocene fossil records of *Palaeocarya* sp. from the Changchang Basin, with an estimated age of 48.6–37.2 Ma (Jin, 2009; Spicer et al., 2014), were used to calibrate the crown age. Additionally, some studies have named these fossils as modern *Engelhardia* based on microcomputed tomography imaging (Huegele and Manchester, 2019; Song et al., 2023). All the fossils were set a lognormal calibration prior, and the MCMC simulations were run with a length of 2.5×10^8 generations, sampled every 10^4 generations. Convergence was assessed using Tracer v1.6 (Rambaut et al., 2014) by analyzing the log files generated by BEAST. The final tree was built using TREEANNOTATOR v2.6.0 (Helfrich et al., 2018) with median node heights, in which the initial 30% of trees was discarded as burn-in.

2.6. Genetic diversity and gene flow

The populations module from Stacks was used to estimate nucleotide diversity (π), expected heterozygosity (He), observed heterozygosity (Ho), and inbreeding coefficients (F_{IS}). To calculate the genetic variation among groups, among populations, and within populations, molecular variance (AMOVA) was conducted using Arlequin v3.11 (Excoffier et al., 2005).

Migration events among populations were inferred using maximum likelihood methods implemented in TreeMix v1.13 (Pickrell and Pritchard, 2012). The software estimated a maximum likelihood tree where migration events among populations were modeled. We allowed up to five migration events, running in the TreeMix algorithm with the -m parameter. The standard errors of all entries in the covariance matrix estimated from the data were used to generate a heatmap. Visualization of the migration tree and heatmap was created using R.

2.7. Demographic histories and species distribution modelling

Stairway Plot v2.1 (Liu and Fu, 2020) was used to explore the dynamics of the effective population size (Ne) of *E. roxburghiana*. We calculated the folded site frequency spectrum (SFS) of the SNPs by the Python script easySFS.py (https://github.com/isaacovercast/easySFS). A common mutation rate of 1.952×10^{-9} per locus and a generation time of 30 years were applied (Bai et al., 2018).

To model the historical and future distribution shifts of *E. roxburghiana*, four periods (Last Glacial Maximum [LGM]; 1970–2000, 2041–2060, and 2080–2100) were selected to estimate its potential distribution range. We downloaded the bioclimatic variables from WorldClim (https://worldclim.org/), and 2.5 arcmin was set in spatial resolution. For future climate projections, we chose the shared socioeconomic pathways SSP245. We subsequently used the 'variance inflation factor' (VIF) function in R package "usdm" (Naimi et al., 2014) to eliminate climate factors with correlation coefficients >0.8, and obtained nine climate factors, including mean diurnal range, isothermality, mean temperature of wettest quarter, mean temperature of driest quarter, mean temperature of warmest quarter, annual precipitation, precipitation of driest month, precipitation seasonality and precipitation of warmest quarter (Table S5). MaxEnt v3.4.4 (Elith et al., 2011; Phillips et al., 2006) was employed for maximum entropy-based modelling. The models were estimated from the average of 10 replicates, in which performance of 25% of the points (to test the model) were estimated and the area under the curve (AUC) of the receiver operating characteristic (ROC) were evaluated. The results of MaxEnt model were visualized in ArcGIS v10.6 (https://www.esri.com/en-us/arcgis/products/index).

3. Results

3.1. Sequence data

After quality control with SOAPnuke, we obtained 778.31 G of clean data (Table S3). The clean data showed an average guanine-cytosine (GC) content of 36.88% and an average Q ≥ 20 rate of 96.86% (Table S3), indicating a high sequencing data quality suitable for subsequent analysis. The mean percentage of RAD reads mapped to the reference genome was 97.09% (Table S4). After filtering, we obtained two datasets for further analysis. The first dataset comprised 242 individuals of *E. roxburghiana* as the ingroup, yielding 23,579 SNPs. The second dataset included eight individuals of *R. chiliantha* as the outgroup, with 14,854 SNPs obtained for phylogenetic analyses.

3.2. Population genetic structure

The analysis using STRUCTURE initially suggested the presence of two distinct genetic lineages, represented by $K = 2$, which was supported by the consideration of ΔK values (Fig. S2). This partitioning separated the sites into two primary clusters based on their geographic distributions: Cluster I encompassed the Truong Son Mountain Range (Vietnam), western Chiang-nan Hilly Range, southern Yunnan-Guizhou Plateau, and north-central Vietnam, and Cluster II included Guangdong and Hainan Island (Fig. S3). However, further analysis with $K = 3$ provided a more detailed resolution of the genetic structure, encompassing a diverse range of geographical regions and environmental gradients. It further separated samples within Cluster I into two subgroups: Cluster I—N, comprising the south Yunnan-Guizhou Plateau, west Chiang-nan Hilly Range, and north-central Vietnam (green in

Fig. 1a, b), and Cluster I—S, encompassing the Truong Son Mts. Range (red in Fig. 1a, b). We selected $K = 3$ based on STRUCTURE analyses and PCA results, which revealed that the species' genetic structure was effectively partitioned into three groups along the first two axes of the PCA. The percentages of variation explained by PC1 and PC2 were 22.39% and 17.42%, respectively. Notably, the distribution of samples across these clusters closely resembled the STRUCTURE result for $K = 3$, with each cluster being represented by a different color in Fig. 1c.

3.3. Phylogenetic analyses and divergence time

The ML and BI trees consisting of 242 *E. roxburghiana* and eight *R. chiliantha* were constructed using IQ-tree and BEAST, exhibited similar topologies and were organized into four distinct clades (Fig. 2a and S4). The initial divergence within *E. roxburghiana* started ca. 52.25 Ma (95% Highest Posterior Density (HPD): 52.06–52.48 Ma; Fig. 2a). The divergence time of cluster I—S occurred at ca. 50.30 Ma (95% HPD: 49.43–51.00 Ma; Fig. 2a). The split between clusters I—N and II occurred at ca. 43.84 Ma (95% HPD: 42.71–45.12 Ma; Fig. 2a). Finally, within cluster II, *E. roxburghiana* of Hainan Island diverged from taxa in Guangdong province starting ca. 37.86 Ma (95% HPD: 37.01–38.92 Ma; Fig. 2a).

3.4. Diversity and gene flow

The nucleotide diversity (π), expected heterozygosity (*He*), and observed heterozygosity (*Ho*) ranged from 0.043 (V01) to 0.326 (G02), 0.038 (V01) to 0.293 (G02), and 0.054 (V01) to 0.32 (G03; Table S1),

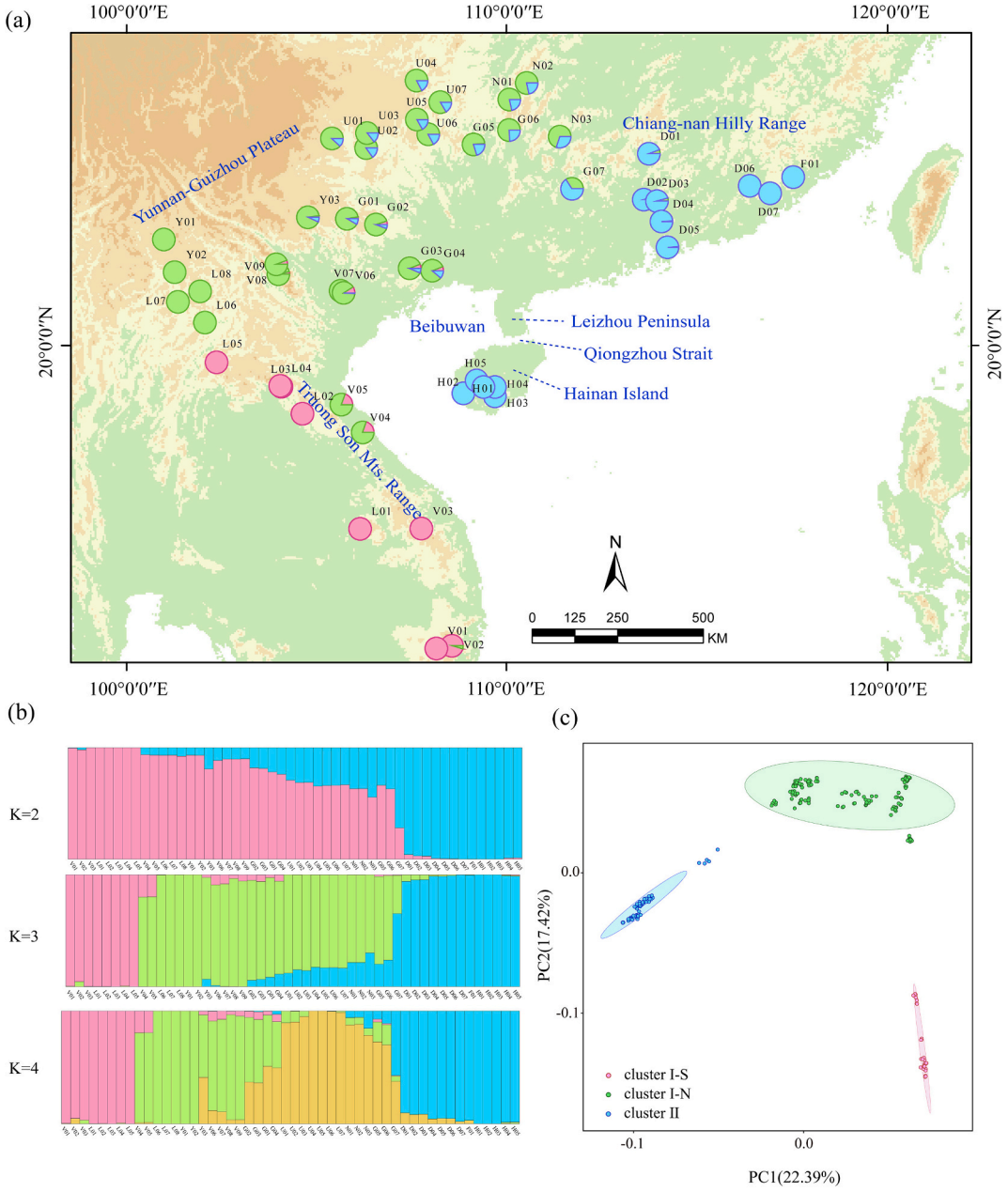

Fig. 1. Geographical distribution and population genetic structure in *E. roxburghiana*. (a) Geographical distribution of the 50 sampled populations and their color-coded grouping according to the structure analysis ($K = 3$). (b) Histogram of the structure analysis for the model with $K = 2$, $K = 3$, and $K = 4$. The *x*-axis shows populations, and the *y*-axis quantifies the proportion of inferred ancestral lineages. (c) Principal component analysis (PCA) is color-coded to indicate different groups of *E. roxburghiana*; red, green, and blue indicate clusters I—S, I—N, and II, respectively. (For interpretation of the references to color in this figure legend, the reader is referred to the web version of this article.)

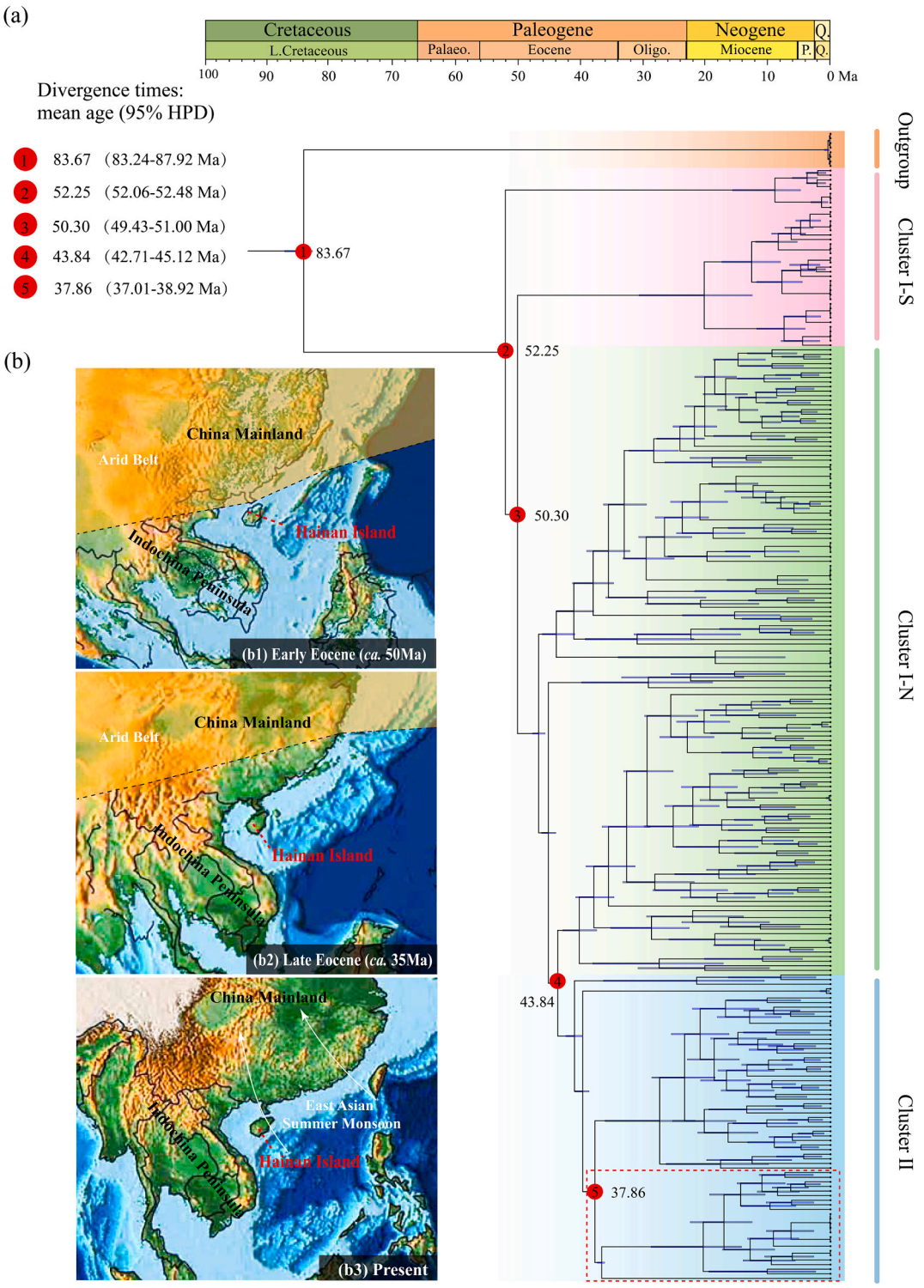

Fig. 2. Chronogram of divergence times and palaeomaps in the Indochina Peninsula and the southern China. (a) Chronogram of *E. roxburghiana* inferred by BEAST. Blue bars represent 95% highest posterior density (HPD) intervals. The red dotted line includes the *E. roxburghiana* in Hainan Island. (b) The palaeomaps of China mainland and Indochina Peninsula obtained from Gplates (http://www.earthbyte.org/paleomap-paleoatlas-for-gplates/) in (b1) the Middle Eocene, (b2) Late Eocene and (b3) the present. The Yellow shading is the arid zone (from Wu et al., 2022). The white arrow is the direction of EASM (from Li et al., 2021). (For interpretation of the references to color in this figure legend, the reader is referred to the web version of this article.)

respectively, across the 50 populations. The inbreeding coefficient (F_{IS}) values were consistently near zero or not significantly different from zero across all locations (Table S1). The percentage of variation among groups, among populations, and within populations, and fixation indices (F_{ST}, F_{SC}, F_{CT}) were reported using AMOVA (Table S2). Specifically, 21.98% of the variation was among the groups, 20.83% was among populations within the groups, and the remaining 57.19% occurred within populations (Table S2).

TreeMix inferred a maximum likelihood phylogenetic population tree, which shared a topology structure similar to those of trees

constructed using IQ-tree and BEAST (Figs. 2a, S4, and S5). Three strong mixed events were inferred: migration from N03 to G07 (migration weight: 0.4324), from U03 to G01 (migration weight: 0.4308), and from V04, V05, V06 and V07 to G04 (migration weight: 0.4191; Table S6). Two weaker migration events were detected: migration from V04 and V05 to cluster II (migration weight: 0.3243) and from U01 to Y03 (migration weight: 0.2988; Table S6).

3.5. Demographic history and species distribution modelling

Changes in Ne were inferred for the three groups using Stairway Plot, revealing fluctuations in Ne during Quaternary glaciations (Fig. 3a). Cluster I—S suffered from a deep bottleneck (approximately 40–4 kya) with two sharp-drop stairstep patterns before and after the LGM, followed by a rapid recovery after the last glacial period (LGP; Fig. 3a1). Cluster II also exhibited a bottleneck (approximately 10–4 kya), with a decline post-LGP and subsequent recovery during 6–5 kya (Fig. 3a3). The Ne of cluster I—N showed a downward trend, experiencing a relatively rapid decline during the LGM (Fig. 3a2). Since the Holocene, both clusters I—N and II have suffered population contractions (Figure 3a2, 3).

The MaxEnt model for *E. roxburghiana* achieved an AUC value of 0.888 ± 0.058 (mean ± SD), indicating high predictive accuracy. Under current bioclimatic conditions, the model projection showed good habitat suitability in Vietnam and southern China (Figure 3b2). During the LGM, the species exhibited a wider distribution compared to its current range, with expansion in the Yunnan-Guizhou Plateau, Shan Plateau, and Chiang-nan Hilly Range (Fig. 3b1). However, the potential species range in Vietnam has contracted slightly (Fig. 3b1). Future climate scenarios predict contraction in the Chiang-nan Hilly Range and expansion in southern China and Hainan Island (Fig. 3b3, 4).

4. Discussion

4.1. Genetic structure and genetic diversity

Our analysis revealed the presence of three distinct regional groups of *E. roxburghiana* spanning the Indochina Peninsula to southern China. Additionally, some admixed populations were observed between the southern Indochina Peninsula and the Chiang-nan Hilly Ranges (Fig. 1a). The lineage composition of Hainan Island was similar to that of the Chiang-nan Hilly Ranges (Fig. 1a), indicating a close genetic relationship. *E. roxburghiana* is distributed along Beibuwan, and even in the Indochina Peninsula; thus, the distribution patterns indicate that Hainan Island was not biologically separated from Beibuwan. Although the floristic composition indicates that Hainan Island has a closer relationship with northern parts of Vietnam and Guangxi (Zhu, 2016), our genetic structure analysis indicates a strong affinity between Hainan Island and Guangdong (Fig. 1a). Furthermore, based on the results of recent studies (Huo et al., 2022; Lin et al., 2021; Ali, 2018), the flora of Hainan Island exhibits a high degree of similarity to those of Vietnam and Guangxi. This is attributed to the formation of numerous land bridges in low-lying areas, which facilitated the dispersal of plants and frequent exchange of floristic elements.

Genetic diversity is a crucial indicator of a population's capacity to evolve and adapt to different environments over time (Wei et al., 2017). In this study, populations in cluster I—N (Fig. 1a), located in the west Chiang-nan Hilly Range and southeast Yunnan-Guizhou Plateau, exhibited higher genetic diversity (Table S1), likely for multiple refugia in these regions. High levels of plant diversity are often linked to mountainous regions due to their climatic and topographic heterogeneity throughout their geological history (Huber et al., 2005; Médail and Diadema, 2009). Mountains in southern China have historically served as refugia during glacial cycles (Wang et al., 2009; López-Pujol et al., 2011; Tian et al., 2018; Liu et al., 2022b; Meng et al., 2022b), providing multiple stable and suitable environments for maintaining genetic diversity in subtropical China (Wang et al., 2009; López-Pujol et al., 2011; Tang et al., 2018). In addition, topographic heterogeneity generates genetic diversity (Ortego et al., 2015), particularly when coupled with orbitally-paced climate change even at low latitudes (Spicer et al., 2024). In this study, the populations in the west Chiang-nan Hilly Range, southeast Yunnan-Guizhou Plateau, and north central Vietnam showed a hybrid zone, indicated by the lineage composition (Fig. 1a). Thus, the mixed populations in the lineage of cluster I—N (e.g., G01, N04, G05, G07; Fig. 1a) are due to genetic introgression from clusters I—S and II, which provide higher genetic diversity for cluster I—N. Meanwhile, significant migration events were primarily observed between populations on the adjacent continent, especially within the mixed populations, but not between the mainland and Hainan Island (Fig. S6). It appears that the divergence time between lineages on the mainland and Hainan Island was extensive. Lower genetic diversity was observed in cluster I—S, primarily located in the Truong Son Mt. Range (Table S1). Furthermore, a severe historical bottleneck was detected in cluster I—S (Fig. 3a1). Bottlenecks often result in a loss of genetic diversity, reducing population viability (Bouzat et al., 1998; Banks et al., 2013), and have been observed in several species (Ehrich et al., 2000; Brown et al., 2013; Parra et al., 2018). A shallower historical bottleneck was detected in cluster II (Fig. 3a3), which indicates that the genetic diversity loss in the lineages of Guangdong province (southern China) and Hainan Island was not severe, and the level fell between clusters I—S and I—N (Fig. 3a3; Table S1).

Overall, the genetic structure of *E. roxburghiana* in the three groups elucidates the relationships among different lineages in the regions and indicates a close affinity between Hainan Island and Chiang-nan. This affinity may account for the biogeographic patterns observed on Hainan Island. The complexity of genetic diversity within *E. roxburghiana* reflects the dynamic interplay of geological and ecological factors, shaping the distribution and adaptation ability of species in diverse landscapes.

4.2. Biogeographic pattern in relation to Hainan Island

Hainan Island is intricately bound to its neighboring mainlands through a web of complex relationships. These interactions, shaped by the island's geological history, climatic fluctuations, and biological migrations, have exerted a profound influence on the island's biota, contributing to its unique ecological dynamics.

In recent years, several studies have speculated that Hainan Island might have experienced a period of drift and used the hypothesized plate tectonic history to explain the origin of its biota (Zhu, 2016, 2017, 2020; Luo and Li, 2017). These studies assumed Hainan Island was situated on the border of China-Vietnam during the Eocene (ca. 56.0–33.9 Ma) and then drifted to the present location. They argue that it was due to the collision between the Indian and Eurasian plates caused the uplift of the Tibetan Plateau and the compression of the Indochina Peninsula Block (Liu et al., 2022a; Li et al., 2024), leading to the movement of Hainan Island. However, the conclusions of our study appear to challenge this speculation. Our data provide no evidence for this drift of Hainan Island. Herein, we integrate genetic structure, molecular dating, and fossil records to reconstruct the biogeographic patterns of Hainan Island and its neighboring landmasses.

Regarding genetic structure, the lineages of *E. roxburghiana* on Hainan Island indicate that Hainan Island and Chiang-nan Hilly Range converge (Fig. 1a), which is shown by *E. roxburghiana* on Hainan Island having a closer affinity to the lineages on Chiang-nan rather than Guangxi or Vietnam. This observation is supported by the divergence times of the lineages and the reconstruction of palaeomaps of mainland China and the Indochina Peninsula obtained from Gplates (http://www.earthbyte.org/paleomap-paleoatlas-for-gplates/). Our findings suggest that Hainan Island was geographically close to Chiang-nan during the early to late Eocene (Fig. 2b1, 2). There was undoubtedly a close biotic affinity between Hainan Island and Chiang-nan, regardless of the number of lineages considered (K = 2 or 3; Figs. 1a and S3).

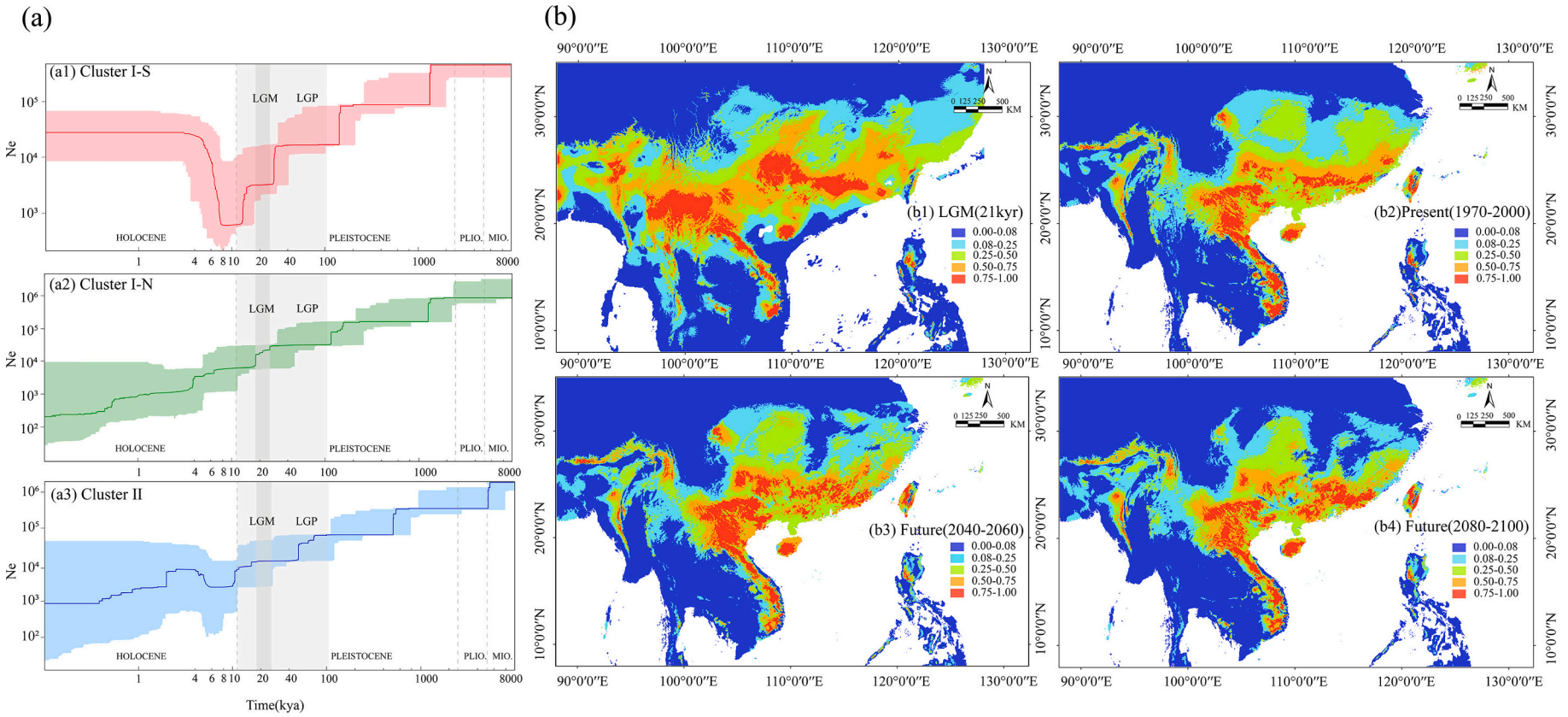

Fig. 3. Demographic history and ecological niche modelling. (a) Demographic history inferred by Stairway Plot for the three groups of *E. roxburghiana*. The *x*-axis indicates time before the present in thousand years ago (kya) on a log scale, and the *y*-axis represents the effective population size. The bold color curve and the light color shaded areas show the median estimate and 95% confidence interval, respectively. The light and dark gray shaded areas indicate the Last Glacial Period (LGP) and the Last Glacial Maximum (LGM), respectively. (a1) cluster I—S, (a2) cluster I—N, (a3) cluster II; (b) Potential distributions as probability of occurrence for *E. roxburghiana* in Hainan Island and adjacent areas. (b1) At the LGM; 21 kya before the present; BP), (b2) under current conditions (1970–2000), (b3) under future conditions (2040–2060), and (b4) under future conditions (2080–2100).

Additionally, the comprehensive genetic structure and the molecular dating, calibrated using fruit fossil records in Hainan Island, confirm that the lineage identified in this study dispersed from Chiang-nan to Hainan Island in the Eocene (Fig. 2a). This evidence refutes the hypothesis that suggests Hainan Island was connected to Vietnam and Guangxi during the Eocene.

Speculations regarding the geographical position of Hainan Island in the Eocene have also been questioned by geologists, because known geological and geophysical data are inconsistent with the notion of Hainan Island drifting from the Asian mainland (Ali, 2018). The high similarity of the biota between Hainan Island and Vietnam is likely due to a land bridge connecting Hainan Island to mainland China and the Indochina Peninsula (Ali, 2018; Lin et al., 2021; Huo et al., 2022). Furthermore, the significant palaeontological and sedimentological congruency has been observed between the Youganwo flora in the Maoming Basin of Guangdong Province and the Changchang flora in the Changchang Basin of Hainan Island, dating back to the late Eocene (Herman et al., 2017; Spicer et al., 2014). This consistent evidence of land connection provides crucial insights into the close palaeogeographical link between Hainan Island and Chiang-nan in the evolution of *E. roxburghiana*, further corroborating our research findings. Herein, explicit fossil records of *E. roxburghiana*, coupled with its extinct distributions in the above-mentioned regions, provide evidence of the broad-scale history and palaeogeography of Hainan Island, producing a framework consistent with the evolution of *E. roxburghiana*. Additionally, sedimentary evidence suggests that marine facies were first established in the northern SCS (i.e., in both the Zhujiangkou Basin and the Qiongdongnan Basin) during the late Eocene to early Oligocene (Jiang et al., 1994). The marine environment did not expand to the Beibuwan Basin until the early Miocene (Wang and Li, 2009). This geological evidence supports our proposal that land bridge in the Beibuwan Basin facilitated the dispersal of *E. roxburghiana* from the mainland to Hainan Island during the late Eocene (Fig. 2b2), which is consistent with our biogeographic deductions. Our results provide new insights into the evolutionary history of Hainan Island's flora and underscore the intricate biogeographic connections between Hainan Island and its surrounding regions.

4.3. Evolutionary trajectory

E. roxburghiana has an expansive range spanning from southern China to the Indochina Peninsula. To elucidate the evolutionary dynamics of this species, we used an integrated approach combining molecular dating techniques, a thorough examination of the fossil record, and historical climatic events. This approach allowed us to identify the key factors influencing the dispersal and colonization route of *E. roxburghiana* across these regions.

The discovery of fruit fossils in the Changchang Basin (Hainan Island) demonstrated that *Engelhardia* occupied Hainan Island during the Eocene (Jin, 2009). We identified four main phylogenetic clades of *E. roxburghiana* using both ML and BI methods (Figs. 2a and S4). These analyses revealed that the earliest divergent clade originated in the southern Indochina Peninsula, situated at low latitudes within the tropic region. The results indicated that *E. roxburghiana* originated in the tropical Indochina Peninsula.

Notably, throughout much of the Paleogene, East Asia was characterized by a vast arid belt in the mid-latitudes (Sun and Wang, 2005; Clift et al., 2008; Xiong et al., 2020). Consequently, during that period, East Asia was not the primary habitat for the moisture-loving species *E. roxburghiana*. The Eocene uplift in eastern Tibet notably intensified seasonal rainfall, leading to the retreat of the arid belt in East Asia and inducing a distinct Eocene Asian climate that significantly differed from the contemporary monsoonal pattern (He et al., 2022). Characterized by bimodal precipitation and a winter-wet regime, this unique Eocene monsoon pattern played a pivotal role in enhancing biodiversity across East Asia (Zhao et al., 2023; He et al., 2022).

Following the demise of the arid zone, the Pan Gulf of Tonkin region, with northern Vietnam as its core, emerged as a significant reservoir for the evolution of East Asian flora (Fig. 2b1, 2; Huang et al., 2022; Li et al., 2021). Furthermore, the uplift of eastern Tibet in the late Eocene led to increased precipitation in East Asia (He et al., 2022). We speculate that the warm and humid climate allowed *E. roxburghiana* to spread northward from the Pan Gulf of Tonkin region to some parts of southern China. During the Miocene, climate in Asia changed from a zonal to monsoon-dominated pattern (Guo et al., 2008; Wu et al., 2022). An important subcomponent of the Asian Monsoon, the East Asian Summer Monsoon (EASM), became the main factor influencing moisture in southern China (Fig. 2b3; Guo et al., 2008; Li et al., 2021; Spicer and Farnsworth, 2021; Wu et al., 2022). The diversification of *E. roxburghiana* in southern China occurred during the Miocene, coinciding with the strengthening precipitation of the EASM (Fig. 2a; Farnsworth et al., 2019). This pattern is consistent with other findings (Meng et al., 2022b), suggesting that the strengthening of the EASM precipitation facilitated the diversification of *E. roxburghiana* in southern China.

During the Quaternary, significant climate fluctuations drove changes in the geographic distribution of *E. roxburghiana*. Given the species' wide geographical range, it responded differently to the environment in the various regions. For example, in the Indochina Peninsula, *E. roxburghiana* experienced a dramatic contraction followed by a rapid expansion after the LGP (Fig. 3a1). Although glacial climates had limited impact on *E. roxburghiana* in southern China, intensive human activities have led to an overall population decline (Fig. 3a2, 3). Presently, the distribution of *E. roxburghiana* has stabilized, forming the current pattern. Analyses of the species' suitable distribution during the LGM and the fluctuations in effective population size reveal a concentration of *E. roxburghiana* in southern China during the LGM, contrasting with its current distribution, which is concentrated in the Indochina Peninsula (Fig. 3a1, b1, 2). We speculate that southern China, particularly in Chiang-nan Hill Range and Yunnan-Guizhou Plateau, served as refugia for *E. roxburghiana* during the Quaternary glaciation. Meanwhile, species in the Indochina Peninsula (i.e., cluster I—S) swiftly recovered and remained stable after the LGP (Fig. 3a1). However, since the Holocene (Walker et al., 2009), populations in southern China (i.e., clusters I—N and II) have experienced mild population declines, which are likely linked to extensive land use, as human activities have been prevalent in southern China for millennia (Fig. 3a2, 3; Liu et al., 2019). MaxEnt models predict that the distribution of *E. roxburghiana* will be concentrated in southern China in the future (Fig. 3b3, 4), indicating its continuing role as a refugium.

5. Conclusions

In summary, our large-scale sampling and RAD-seq data of *E. roxburghiana* provide insights into the palaeogeography of Hainan Island and adjacent mainland areas. Biogeographic patterns of *E. roxburghiana* reveal that Hainan Island was in close biotic contact with Chiang-nan during the Eocene (Fig. 2b1), and *E. roxburghiana* spread to Hainan Island from Chiang-nan via a land bridge during the late Eocene (Fig. 2b2). Consequently, we challenge the hypothesis suggesting a connection between Hainan Island and Vietnam, as well as Guangxi, existed during the Eocene. The distribution area of *E. roxburghiana* expanded northward with the retreat of an arid belt on mainland Asia (Fig. 2b1, 2), and higher precipitation during the Miocene and the modern EASM ultimately facilitated the diversification of *E. roxburghiana*. Moreover, the different trajectories of three groups in effective population size and species distribution modelling indicate a refugium in southern China during the Quaternary glaciations and in the future (Fig. 3). Considering geological data relating to Hainan Island and our biogeographic patterns, we do not believe that Hainan Island is a wandering microplate. Our study rejects the proposed hypotheses of the drift of Hainan Island; however, this should be further verified by more

studies on other organisms that demonstrate similar biogeographic patterns.

CRediT authorship contribution statement

Pei-Han Huang: Writing – review & editing, Writing – original draft, Visualization, Software, Methodology. **Tian-Rui Wang:** Software, Methodology. **Min Li:** Writing – review & editing, Conceptualization. **Zi-Jia Lu:** Methodology. **Ren-Ping Su:** Writing – original draft. **Ou-Yan Fang:** Writing – original draft. **Lang Li:** Investigation. **Shi-Shun Zhou:** Investigation. **Yun-Hong Tan:** Writing – original draft, Investigation. **Hong-Hu Meng:** Writing – review & editing, Writing – original draft, Visualization, Supervision, Project administration, Investigation, Funding acquisition, Conceptualization. **Yi-Gang Song:** Writing – review & editing, Writing – original draft, Funding acquisition, Conceptualization. **Jie Li:** Writing – original draft, Conceptualization.

Declaration of competing interest

The authors declare no conflicts of interest.

Data availability

Data will be made available on request.

Acknowledgements

We'd like to thank Prof. Robet A. Spicer for his insightful suggestions and comments on the manuscript, which improved the manuscript and made the manuscript more readable. This study was supported by the National Natural Science Foundation of China (No. 42171063); Southeast Asia Biodiversity Research Institute, Chinese Academy of Sciences (No. Y4ZK111B01); the Special Fund for Scientific Research of Shanghai Landscaping and City Appearance Administrative Bureau (G242414, G242416); the "Yunnan Revitalization Talent Support Program" in Yunnan Province (XDYC-QNRC-2022-0028); Yunnan Revitalization Talent Support Program "Innovation Team" Project (202405AS350019); the CAS "Light of West China" Program; and the 14th Five-Year Plan of Xishuangbanna Tropical Botanical Garden, Chinese Academy Sciences (XTBG-1450101). Finally, the reviewers are grateful for the valuable suggestions and comments that help to improve the quality of this study.

Appendix A. Supplementary data

Supplementary data to this article can be found online at https://doi.org/10.1016/j.palaeo.2024.112392.

References

Ali, J.R., 2018. New explanation for elements of Hainan Island's biological assemblage may stretch things a little too far. Ecography 41, 457–460. https://doi.org/10.1111/ecog.03199.

Bai, W.N., Yan, P.C., Zhang, B.W., Woeste, K.E., Lin, K., Zhang, D.Y., 2018. Demographically idiosyncratic responses to climate change and rapid Pleistocene diversification of the walnut genus *Juglans* (Juglandaceae) revealed by whole-genome sequences. New Phytol. 217, 1726–1736. https://doi.org/10.1111/nph.14917.

Banks, S.C., Cary, G.J., Smith, A.L., Davies, I.D., Driscoll, D.A., Gill, A.M., Lindenmayer, D.B., Peakall, R., 2013. How does ecological disturbance influence genetic diversity? Trends Ecol. Evol. 28, 670–679. https://doi.org/10.1016/j.tree.2013.08.005.

Barreda, V.D., Zamaloa, M.D.C., Gandolfo, M.A., Jaramillo, C., Wilf, P., 2020. Early eocene spore and pollen assemblages from the laguna del hunco fossil lake beds, Patagonia, Argentina. Int. J. Plant Sci. 181, 594–615. https://doi.org/10.1086/708386.

Bosch, N.E., Espino, F., Tuya, F., Haroun, R., Bramanti, L., Otero-Ferrer, F., 2023. Black coral forests enhance taxonomic and functional distinctiveness of mesophotic fishes in an oceanic island: Implications for biodiversity conservation. Sci. Rep. 13, 4963. https://doi.org/10.1038/s41598-023-32138-x.

Bouckaert, R., Heled, J., Kühnert, D., Vaughan, T., Wu, C.H., Xie, D., et al., 2014. BEAST 2: A software platform for Bayesian evolutionary analysis. PLoS Comput. Biol. 10, e1003537 https://doi.org/10.1371/journal.pcbi.1003537.

Bouzat, J.L., Cheng, H.H., Lewin, H.A., Westemeier, R.L., Brawn, J.D., Paige, K.N., 1998. Genetic evaluation of a demographic bottleneck in the greater prairie Chicken. Conserv. Biol. 12, 836–843. https://doi.org/10.1111/j.1523-1739.1998.97164.x.

Brown, S.M., Harrisson, K.A., Clarke, R.H., Bennett, A.F., Sunnucks, P., 2013. Limited population structure, genetic drift and bottlenecks characterise an endangered bird species in a dynamic, fire-prone ecosystem. PLoS One 8, e59732. https://doi.org/10.1371/journal.pone.0059732.

Catchen, J., Hohenlohe, P.A., Bassham, S., Amores, A., Cresko, W.A., 2013. Stacks: An analysis tool set for population genomics. Mol. Ecol. 22, 3124–3140. https://doi.org/10.1111/mec.12354.

Chen, G.D., 1956. Examples of Chinese platform and discussions of "Cathaysia". Acta Geol. Sin. 36, 239–271. https://doi.org/10.19762/j.cnki.dizhixuebao.1956.03.001.

Chen, Y., Chen, Y.S., Shi, C.M., Huang, Z., Zhang, Y., Li, S.K., Li, Y., Ye, J., Yu, C., Li, Z., Zhang, X.Q., Wang, J., Yang, H.M., Fang, L., Chen, Q., 2017. SOAPnuke: A MapReduce acceleration-supported software for integrated quality control and preprocessing of high-throughput sequencing data. GigaScience 7. https://doi.org/10.1093/gigascience/gix120.

Chen, Z., Zhou, Z., Guo, Z.M., Van Do, T., Sun, H., Niu, Y., 2023. Historical development of karst evergreen broadleaved forests in East Asia has shaped the evolution of a hemiparasitic genus Brandisia (Orobanchaceae). Plant Divers. 45, 501–512. https://doi.org/10.1016/j.pld.2023.03.005.

Clift, P.D., Hodges, K.V., Heslop, D., Hannigan, R., Long, H.V., Calves, G., 2008. Correlation of himalayan exhumation rates and asia monsoon intensity. Nat. Geosci. 1, 875–880. https://doi.org/10.1038/ngeo351.

Cox, C.B., Moore, P.D., Ladle, R., 2016. Biogeography: An Ecological and Evolutionary Approach, 9th edition.

Danecek, P., Auton, A., Abecasis, G., Albers, C.A., Banks, E., DePristo, M.A., et al., 2011. The variant call format and VCFtools. Bioinformatics 27, 2156–2158. https://doi.org/10.1093/bioinformatics/btr330.

Darriba, D., Taboada, G.L., Doallo, R., Posada, D., 2012. jModelTest 2: More models, new heuristics and parallel computing. Nat. Methods 9, 772. https://doi.org/10.1038/nmeth.2109.

Darwin, C., 1859. On the Origin of Species. John Murray, London.

Ding, Y.M., Pang, X.X., Cao, Y., Zhang, W.P., Renner, S.S., Zhang, D.Y., Bai, W.N., 2023. Genome structure-based Juglandaceae phylogenies contradict alignment-based phylogenies and substitution rates vary with DNA repair genes. Nat. Commun. 14, 617. https://doi.org/10.1038/s41467-023-36247-z.

Doyle, J.J., Doyle, J.L., 1987. A rapid DNA isolation procedure forsmall quantities of fresh leaf tissue. Phytochem. Bullet. 19, 11–15.

Earl, D.A., vonHoldt, B.M., 2012. Structure harvester: A website and program for visualizing structure output and implementing the Evanno method. Conserv. Genet. Resour. 4, 359–361. https://doi.org/10.1007/s12686-011-9548-7.

Ehrich, D., Fedorov, V.B., Stenseth, N.C., Krebs, C.J., Kenney, A., 2000. Phylogeography and mitochondrial DNA (mtDNA) diversity in north American collared lemmings (*Dicrostonyx groenlandicus*). Mol. Ecol. 9, 329–337. https://doi.org/10.1046/j.1365-294x.2000.00853.x.

Elith, J., Phillips, S.J., Hastie, T., Dudı'k, M., Chee, Y.E., Yates, C.J., 2011. A statistical explanation of maxent for ecologists. Divers. Distrib. 17, 43–57. https://doi.org/10.1111/j.1472-4642.2010.00725.x.

Emerson, B.C., 2008. Speciation on islands: What are we learning? Biol. J. Linn. Soc. 95, 47–52. https://doi.org/10.1111/j.1095-8312.2008.01091.x.

Evanno, G., Regnaut, S., Goudet, J., 2005. Detecting the number of clusters of individuals using the software structure: A simulation study. Mol. Ecol. 14, 2611–2620. https://doi.org/10.1111/j.1365-294X.2005.02553.x.

Excoffier, L., Laval, G., Schneider, S., 2005. Arlequin (version 3.0): An integrated software package for population genetics data analysis. Evol. Bioinforma. 1, 47–50.

Farnsworth, A., Lunt, D.J., Robinson, S.A., Valdes, P.J., Roberts, W.H.G., Clift, P.D., Markwick, P.J., Su, T., Wrobel, N., Bragg, F., Kelland, S.J., Pancost, R.D., 2019. Past East Asian monsoon evolution controlled by paleogeography, not CO2. Sci. Adv. 5, eaax1697. https://doi.org/10.1126/sciadv.aax1697.

Gillespie, R.G., 2015. Island time and the interplay between ecology and evolution in species diversification. Evol. Appl. 9, 53–73. https://doi.org/10.1111/eva.12302.

Graham, N.R., Gruner, D.S., Lim, J.Y., Gillespie, R.G., 2017. Island ecology and evolution: Challenges in the Anthropocene. Environ. Conserv. 44, 323–335. https://doi.org/10.1017/S0376892917000315.

Guo, Z.T., Sun, B., Zhang, Z.S., Peng, S.Z., Xiao, G.Q., Ge, J.Y., Hao, Q.Z., Qiao, Y.S., Liang, M.Y., Liu, J.F., Yin, Q.Z., Wei, J.J., 2008. A major reorganization of Asian climate by the early Miocene. Clim. Past 4, 153–174. https://doi.org/10.5194/cp-4-153-2008.

He, S.L., Ding, L., Xiong, Z.Y., Spicer, R.A., Farnsworth, A., Valdes, P.J., Wang, C., Cai, F. L., Wang, H.Q., Sun, Y., Zeng, D., Xie, J., Yue, Y.H., Zhao, C.Y., Song, P.P., Wu, C., 2022. A distinctive Eocene Asian monsoon and modern biodiversity resulted from the rise of Eastern Tibet. Sci. Bull. 67, 2245–2258. https://doi.org/10.1016/j.scib.2022.10.006.

Helfrich, P., Rieb, E., Abrami, G., et al., 2018. TreeAnnotator: versatile visual annotation of hierarchical text relations. In: International Conference on Language Resources and Evaluation.

Helmus, M.R., Mahler, D.L., Losos, J.B., 2014. Island biogeography of the Anthropocene. Nature 513, 543–546. https://doi.org/10.1038/nature13739.

Herman, A.B., Spicer, R.A., Aleksandrova, G.N., Yang, J., Kodrul, T., Masolva, N.P., Spicer, T.E.V., Chen, G., Jin, J.J., 2017. Eocene-Oligocene climate and vegetation change in southern China: Evidence from the Maoming Basin. Palaeogeogr.

Palaeoclimatol. Palaeoecol. 479, 126–137. https://doi.org/10.1016/j.palaeo.2017.04.023.
Heřmanová, Z., Kvaček, J., Friis, E.M., 2011. *Budvaricarpus serialis* Knobloch & Mai, an unusual new member of the Normapolles complex from the late cretaceous of the Czech Republic. Int. J. Plant Sci. 172, 285–293. https://doi.org/10.1086/657278.
Hermsen, E.J., Gandolfo, M.A., 2016. Fruits of Juglandaceae from the Eocene of South America. Syst. Bot. 41, 316–328. https://doi.org/10.1600/036364416X691830.
Hirschfeld, M., Barnett, A., Sheaves, M., Dudgeon, C., 2023. What Darwin could not see: Island formation and historical sea levels shape genetic divergence and island biogeography in a coastal marine species. Heredity 131, 189–200. https://doi.org/10.1038/s41437-023-00635-4.
Hou, W., 1992. Basic characteristics of crustal evolution in Hainan Island, China. Geotect. Metalloge. 16, 131–140. https://doi.org/10.16539/j.ddgzyckx.1992.02.004.
Huang, Z., Chiba, H., Fan, X., 2019. The third species of *Darpa* Moore, 1865 in China and some notes on the Genus (Hesperiidae: Pyrginae: Tagiadini). Entomol. News 128, 284–292. https://doi.org/10.3157/021.128.0308.
Huang, J., Spicer, R.A., Li, S.F., Liu, J., Do, T.V., Nguyen, H.B., Zhou, Z.K., Su, T., 2022. Long-term floristic and climatic stability of northern Indochina: Evidence from the Oligocene Ha Long flora, Vietnam. Palaeogeogr. Palaeoclimatol. Palaeoecol. 593, 110930 https://doi.org/10.1016/j.palaeo.2022.110930.
Huang, P.H., Wang, T.R., Li, M., Fang, O.Y., Su, R.P., Meng, H.H., Song, Y.G., Li, J., 2024. Different reference genomes determine different results: Comparing SNP calling in RAD-seq of *Engelhardia roxburghiana* using different reference genomes. Plant Sci. 344, 112109 https://doi.org/10.1016/j.plantsci.2024.112109.
Huber, U.M., Bugmann, H.K.M., Reasoner, M.A., 2005. Global Change and Mountain Regions. An Overview of Current Knowledge. Springer, Dordrecht, The Netherlands.
Huegele, I.B., Manchester, S.R., 2019. Newly recognized diversity of fruits and seeds from the late Paleogene flora of Trinity County, East Texas, USA. Int. J. Plant Sci. 180, 681–708. https://doi.org/10.1086/704358.
Huo, X.J., Yang, Z., Xie, Y.F., Yang, Y., 2022. Tempo and mode of floristic exchanges between Hainan Island and mainland Asia: A case study of the *Persea* Group (Lauraceae). Forests 1722. https://doi.org/10.3390/f13101722.
Jiang, Z., Zeng, L., Li, M., Zhong, Q., 1994. The North Continental Shelf Region of South China Sea. In: Tertiary in Petroliferous Regions of China, vol. 8. Petroleum Industry Press, Beijing, p. 145 (in Chinese).
Jin, J., 2009. Two Eocene fossil fruits from the Changchang Basin of Hainan Island, China. Rev. Palaeobot. Palynol. 153, 150–152. https://doi.org/10.1016/j.revpalbo.2008.07.010.
Jin, J., Kodrul, T.M., Liao, W., et al., 2009. A new species of *Craigia* from the eocene changchang formation of Hainan Island, China. Rev. Palaeobot. Palynol. 155, 80–82. https://doi.org/10.1016/j.revpalbo.2009.02.003.
Kassambara, A., Mundt, F., 2020. Factoextra: Extract and visualize the results of multivariate data analyses. R Pack. Vers. 1.0.7. https://CRAN.R-project.org/package=factoextra.
Lambeck, K., Esat, T.M., Potter, E.K., 2002. Links between climate and sea levels for the past three million years. Nature 419, 199–206. https://doi.org/10.1038/nature01089.
Lamichhaney, S., Berglund, J., Almén, M.S., Maqbool, K., Grabherr, M., Martinez-Barrio, A., Promerova, M., Rubin, C.J., Wang, C., Zamani, N., Grant, B.R., Grant, P. R., Webster, M.T., Andersson, L., 2015. Evolution of Darwin's finches and their beaks revealed by genome sequencing. Nature 518, 371–375. https://doi.org/10.1038/nature14181.
Lê, S., Josse, J., Husson, F., 2008. FactoMineR: An R package for multivariate analysis. J. Stat. Softw. 25, 1–18.
Li, H., 2013. Aligning sequence reads, clone sequences and assembly contigs with BWA-MEM. arXiv preprint arXiv:13033997. https://doi.org/10.48550/arXiv.1303.3997.
Li, H., Durbin, R., 2009. Fast and accurate short read alignment with Burrows–Wheeler transform. Bioinformatics 25, 1754–1760. https://doi.org/10.1093/bioinformatics/btp324.
Li, H., Handsaker, B., Wysoker, A., Fennell, T., Ruan, J., Homer, N., Marth, G., Abecasis, G., Durbin, R., 1000 Genome Project Data Processing Subgroup, 2009. The sequence alignment/map format and SAMtools. Bioinformatics 25, 2078–2079. https://doi.org/10.1093/bioinformatics/btp352.
Li, S.F., Valdes, P.J., Farnsworth, A., Barnard, T.D., Su, T., Liu, J., Lunt, D.J., Spicer, R.A., Liu, J., Deng, W.Y.D., Huang, J., Tang, H., Ridgwell, A., Chen, L.L., Zhou, Z.K., 2021. Orographic evolution of northern Tibet shaped vegetation and plant diversity in eastern Asia. Sci. Adv. 7, eabc7741. https://doi.org/10.1126/sciadv.abc7741.
Li, S.H., Spicer, R.A., Su, T., Zhou, Z.K., Deng, C.L., 2024. An updated chronistratigraphic framework for the Cenozoic sediments of southeast margin of the Tibetan Plateau: Implications for regional tectonics. Glob. Planet. Chang. 236, 104436 https://doi.org/10.1016/j.gloplacha.2024.104436.
Liang, G.H., 2013. Eight evidences about Hainan Island separated from China's Beibu Gulf with drifting and rotation. Acta Geol. Sin. 87, 73–76.
Liang, G.H., 2018. A study of the genesis of Hainan Island. Geol. China 45, 693–705.
Liang, B., Zhou, R.B., Liu, Y.L., Chen, B., Grismer, L.L., Wang, N., 2018. Renewed classification within *Goniurosaurus* (Squamata: Eublepharidae) uncovers the dual roles of a continental island (Hainan) in species evolution. Mol. Phylogenet. Evol. 127, 646–654. https://doi.org/10.1016/j.ympev.2018.06.011.
Lin, X.D., Zong, Y.Q., 1987. More on the origin of the Qiongzhou Strait. Trop. Geogr. Quart. 7, 338–345. https://doi.org/10.13284/j.cnki.rddl.001932.
Lin, S.L., Chen, L., Peng, W.X., Yu, J.H., He, J.K., Jiang, H.S., 2021. Temperature and historical land connectivity jointly shape the floristic relationship between Hainan Island and the neighbouring landmasses. Sci. Total Environ. 769, 144629 https://doi.org/10.1016/j.scitotenv.2020.144629.
Liu, X., Fu, Y.X., 2020. Stairway Plot 2: Demographic history inference with folded SNP frequency spectra. Genome Biol. 21, 280. https://doi.org/10.1186/s13059-020-02196-9.
Liu, J.J., Coomes, D.A., Gibson, L., Hu, G., Liu, J.L., Luo, Y.Q., Wu, C.P., Yu, M.J., 2019. Forest fragmentation in China and its effect on biodiversity. Biol. Rev. 94, 1636–1657. https://doi.org/10.1111/brv.12519.
Liu, J., Milne, R.I., Zhu, G.F., Spicer, R.A., Wambulwa, M.C., Wu, Z.Y., Boufford, D.E., Luo, Y.H., Provan, J., Yi, T.S., Cai, J., Wang, H., Gao, L.M., Li, D.Z., 2022a. Name and scale matter: Clarifying the geography of Tibetan Plateau and adjacent mountain regions. Glob. Planet. Chang. 215, 103893 https://doi.org/10.1016/j.gloplacha.2022.103893.
Liu, X., Zhang, S.Z., Cai, Z.Y., Kuang, Z.R., Wan, N., Wang, Y.J., Mao, L.Y., An, X., Li, F., Feng, T., Liang, X.L., Qiao, Z.L., Nevo, E., Li, K.X., 2022b. Genomic insights into zokors' phylogeny and speciation in China. Proc. Natl. Acad. Sci. USA 119, e2121819119. https://doi.org/10.1073/pnas.2121819119.
Liu, X., Cai, H.M., Wang, W.Q., Lin, W., Su, Z.W., Ma, H.H., 2023. Why is the beautyberry so colourful? Evolution, biogeography, and diversification of fruit colours in *Callicarpa* (Lamiaceae). Plant Divers. 45, 6–19. https://doi.org/10.1016/j.pld.2022.10.002.
López-Pujol, J., Zhang, F.M., Sun, H.Q., Ying, T.S., Ge, S., 2011. Mountains of Southern China as "Plant Museums" and "Plant Cradles": Evolutionary and conservation insights. Mt. Res. Dev. 31, 261–269. https://doi.org/10.1659/MRD-JOURNAL-D-11-00058.1.
Losos, J.B., Ricklefs, R.E., 2009. Adaptation and diversification on islands. Nature 457, 830–836. https://doi.org/10.1038/nature07893.
Lu, A.M., Stone, D.E., Grauke, L.J., 1999. Juglandaceae. In: Wu, Z.Y., Raven, P.H., Hong, D.Y. (Eds.), Flora of China, 4. Science Press; St. Louis: Missouri Botanical Garden Press, Beijing, pp. 278–280.
Luo, Y.F., Li, S.Q., 2017. Cave *Stedocys* spitting spiders illuminate the history of the Himalayas and Southeast Asia. Ecography 41, 414–423. https://doi.org/10.1111/ecog.02908.
Manchester, S.R., 1987. The fossil history of the Juglandaceae. Ann. Mo. Bot. Gard. 21, 1–137. https://doi.org/10.5962/bhl.title.154222.
Manchester, S.R., Collinson, M.E., Goth, K., 1994. Fruits of the Juglandaceae from the Eocene of Messel, Germany, and implications for early tertiary phytogeographic exchange between Europe and western North America. Int. J. Plant Sci. 155, 388–394. https://doi.org/10.1086/297176.
Matthews, T.J., Triantis, K., 2017. Island biogeography. Curr. Biol. 31, 1201–1207.
Médail, F., Diadema, K., 2009. Glacial refugia influence plant diversity patterns in the Mediterranean Basin. J. Biogeogr. 36, 1333–1345. https://doi.org/10.1111/j.1365-2699.2008.02051.x.
Meng, H.H., Song, Y.G., 2023. Biogeographic patterns in Southeast Asia: Retrospectives and perspectives. Biodivers. Conserv. 31, 23261. https://doi.org/10.17520/biods.2023261.
Meng, H.H., Su, T., Huang, Y.J., Zhu, H., Zhou, Z.K., 2015. Late Miocene *Palaeocarya* (Engelhardieae: Juglandaceae) from Southwest China and its biogeographic implications. J. Syst. Evol. 53, 499–511. https://doi.org/10.1111/jse.12145.
Meng, H.H., Zhang, C.Y., Low, S.L., Li, L., Shen, J.Y., Nurainas, Zhang, Huang, P.H., Zhou, S.S., Tan, Y.H., Li, J., 2022a. Two new species from Sulawesi and Borneo facilitate phylogeny and taxonomic revision of *Engelhardia* (Juglandaceae). Plant Divers. 44, 552–564. https://doi.org/10.1016/j.pld.2022.08.003.
Meng, H.H., Zhang, C.Y., Song, Y.G., Yu, X.Q., Cao, G.L., Li, L., Cai, C.N., Xiao, J.H., Zhou, S.S., Tan, Y.H., Li, J., 2022b. Opening a door to the spatiotemporal history of plants from the tropical Indochina Peninsula to subtropical China. Mol. Phylogenet. Evol. 171, 107458 https://doi.org/10.1016/j.ympev.2022.107458.
Mo, Y.Q., Shi, Y.S., 1987. Palaeomagnatic study and tectonic evolution of Hainan Terrane and its vicinal continental coast the late Mesozoic to Cenozoic. J. Nanjing Univ. 23, 521–532.
Myers, N., Mittermeier, R.A., Mittermeier, C.G., et al., 2000. Biodiversity hotspots for conservation priorities. Nature 403, 853–858.
Naimi, B., Hamm, N.A., Groen, T.A., Skidmore, A.K., Toxopeus, A.G., 2014. Where is positional uncertainty a problem for species distribution modelling? Ecography 37, 191–203. https://doi.org/10.1111/j.1600-0587.2013.00205.x.
Nguyen, L.T., Schmidt, H.A., Von Haeseler, A., Minh, B.Q., 2015. IQ-TREE: A fast and effective stochastic algorithm for estimating maximum-likelihood phylogenies. Mol. Biol. Evol. 32, 268–274. https://doi.org/10.1093/molbev/msu300.
Nogué, S., de Nascimento, L., Froyd, C.A., Wilmshurst, J.M., De Boer, E.J., Coffey, E.E.D., Whittaker, R.J., Fernández-Palacios, J.M., Willis, K.J., 2017. Island biodiversity conservation needs palaeoecology. Nat. Ecol. Evol. 1, 181. https://doi.org/10.1038/s41559-017-0181.
Ortego, J., Gugger, P.F., Sork, V.L., 2015. Climatically stable landscapes predict patterns of genetic structure and admixture in the californian canyon live oak. J. Biogeogr. 42, 328–338. https://doi.org/10.1111/jbi.12419.
Parra, G.J., Cagnazzi, D., Jedensjö, M., Ackermann, C.Y., Frère, C.H., Seddon, J.M., Nikolic, N., Krützen, M., 2018. Low genetic diversity, limited gene flow and widespread genetic bottleneck effects in a threatened dolphin species, the Australian humpback dolphin. Conserv. Biol. 220, 192–200. https://doi.org/10.1016/j.biocon.2017.12.028.
Phillips, S.J., Anderson, R.P., Schapire, R.E., 2006. Maximum entropy modeling of species geographic distributions. Ecol. Model. 190, 231–259. https://doi.org/10.1016/j.ecolmodel.2005.03.026.
Pickrell, J.K., Pritchard, J.K., 2012. Inference of population splits and mixtures from genome-wide allele frequency data. PLoS Genet. 8, e1002967 https://doi.org/10.1371/journal.pgen.1002967.

Pritchard, J.K., Stephens, M., Donnelly, P., 2000. Inference of population structure using multilocus genotype data. Genetics 155, 945–959. https://doi.org/10.1093/genetics/155.2.945.

Purcell, S., Neale, B., Todd-Brown, K., Thomas, L., Ferreira, M.A.R., Bender, D., Maller, J., Sklar, P., de Bakker, P.I.W., Daly, M.J., Sham, P.C., 2007. PLINK: A tool set for whole-genome association and population-based linkage analyses. Am. J. Hum. Genet. 81, 559–575. https://doi.org/10.1086/519795.

R Core Team, 2022. R: A Language and Environment for Statistical Computing. R Foundation for Statistical Computing, Vienna, Austria.

Rambaut, A., Suchard, M., Xie, D., Drummond, A., 2014. Tracer v1.6. See. http://beast.bio.ed.ac.uk/Tracer.

Shaw, K.L., Gillespie, R.G., 2016. Comparative phylogeography of oceanic archipelagos: Hotspots for inferences of evolutionary process. Proc. Natl. Acad. Sci. USA 113, 7986–7993. https://doi.org/10.1073/pnas.1601078113.

Shi, M.C., Chen, C.S., Xu, Q.C., Lin, H.C., Liu, G.M., Wang, H., Wang, F., Yan, J.H., 2002. The role of qiongzhou strait in the seasonal variation of the South China Sea circulation. J. Phys. Oceanogr. 32, 103–121. https://doi.org/10.1175/1520-0485(2002)032<0103:TROQSI>2.0.CO;2.

Song, H.Z., Huang, L.L., Xiang, H.L., Quan, C., Jin, J.H., 2023. First reliable Miocene fossil winged fruits record of *Engelhardia* in Asia through anatomical investigation. iScience 26, 106867. https://doi.org/10.1016/j.isci.2023.106867.

Spicer, R.A., Farnsworth, A., 2021. Progress and challenges in understanding Asian palaeogeography and monsoon evolution from the perspective of the plant fossil record. J. Paleontol. 70, 213–235. https://doi.org/10.54991/jop.2021.16.

Spicer, R.A., Herman, A.B., Liao, W.B., Spicer, T.E.V., Kodrul, T.M., Yang, J., Jin, J.H., 2014. Cool tropics in the Middle Eocene: Evidence from the Changchang Flora, Hainan Island, China. Palaeogeogr. Palaeoclimatol. Palaeoecol. 412, 1–16. https://doi.org/10.1016/j.palaeo.2014.07.011.

Spicer, R.A., Farnsworth, A., Su, T., et al., 2024. The progressive co-evolutionary development of the pan-tibetan highlands, the Asian monsoon system and asian biodiversity. Geological Society of London special Papers. Geol. Soc. Spec. Publ. 549 https://doi.org/10.1144/SP549-2023-180.

Sun, X.J., Wang, P.X., 2005. How old is the asian monsoon system? Palaeobotanical records from China. Palaeogeogr. Palaeoclimatol. Palaeoecol. 222, 181–222. https://doi.org/10.1016/j.palaeo.2005.03.005.

Tang, C.Q., Matsui, T., Ohashi, H., Dong, Y.F., Momohara, A., Herrando-Moraira, S., et al., 2018. Identifying long-term stable refugia for relict plant species in East Asia. Nat. Commun. 9, 4488. https://doi.org/10.1038/s41467-018-06837-3.

Tian, S., Kou, Y.X., Zhang, Z.R., Yuan, L., Li, D.R., López-Pujol, J., Fan, D.M., Zhang, Z.Y., 2018. Phylogeography of *Eomecon chionantha* in subtropical China: The dual roles of the Nanling Mountains as a glacial refugium and a dispersal corridor. BMC Evol. Biol. 18, 20. https://doi.org/10.1186/s12862-017-1093-x.

Walker, M., Johnsen, S.J., Rasmussen, S.O., et al., 2009. Formal definition and dating of the GSSP (Global Stratotype Section and Point) for the base of the Holocene using the Greenland NGRIP ice core, and selected auxiliary records. J. Quat. Sci. 24, 3–17. https://doi.org/10.1002/jqs.1227.

Wallace, A.R., 1860. On the zoological geography of the Malay Archipelago. J. Linn. Soc. 4, 172–184. https://doi.org/10.1111/j.1096-3642.1860.tb00090.x.

Wang, P.X., Li, Q.Y., 2009. The South China Sea: Paleoceanography and Sedimentology, vol. 13. Springer, New York, NY.

Wang, J., Gao, P., Kang, M., et al., 2009. Refugia within refugia: The case study of a canopy tree (*Eurycorymbus cavaleriei*) in subtropical China. J. Biogeogr. 36, 2156–2164. https://doi.org/10.1111/j.1365-2699.2009.02165.x.

Wei, X.Z., Bao, D.C., Meng, H.J., Jiang, M.X., 2017. Pattern and drivers of species-genetic diversity correlation in natural forest tree communities across a biodiversity hotspot. J. Plant Ecol. 11, 761–770. https://doi.org/10.1093/jpe/rtx046.

Whittaker, R.J., Fernández-Palacios, J.M., 2007. Island Biogeography: Ecology, Evolution, and Conservation. Oxford University Press, Oxford.

Whittaker, R.J., Fernández-Palacios, J.M., Matthews, T.J., Borregaard, M.K., Triantis, K. A., 2017. Island biogeography: Taking the long view of nature's laboratories. Science 357, eaam8326. https://doi.org/10.1126/science.aam8326.

Wickham, H., 2016. ggplot2: Elegant Graphics for Data Analysis. Springer, New York.

Wilf, P., 2012. Rainforest conifers of Eocene Patagonia: Attached cones and foliage of the extant Southeast Asian and Australasian genus *Dacrycarpus* (Podocarpaceae). Am. J. Bot. 99, 562–584. https://doi.org/10.3732/ajb.1100367.

Wu, F.L., Fang, X.M., Yang, Y., Dupont-Nivet, G., Nie, J.S., Fluteau, F., Zhang, T., Han, W. X., 2022. Reorganization of asian climate in relation to Tibetan Plateau uplift. Nat. Rev. Earth Environ. 3, 684–700. https://doi.org/10.1038/s43017-022-00331-7.

Xiong, Z.Y., Ding, L., Spicer, R.A., Farnsworth, A., Wang, X., Valdes, P.J., Su, T., Zhang, L. Y., Cai, F.L., Wang, H.Q., Li, Z.Y., Song, P.P., Guo, X.D., Yue, Y.H., 2020. The early Eocene rise of the Gonjo Basin, SE Tibet: From low desert to high forest. Earth Planet. Sci. Lett. 543, 116312 https://doi.org/10.1016/j.epsl.2020.116312.

Zhang, C.Y., Low, S.L., Song, Y.G., Nurainas, Kozlowski, Li, L., Zhou, S.S., Tan, Y.H., Cao, G.L., Zhou, Z., Meng, H.H., Li, J., 2020. Shining a light on species delimitation in the tree genus *Engelhardia* Leschenault ex Blume (Juglandaceae). Mol. Phylogenet. Evol. 152, 106918 https://doi.org/10.1016/j.ympev.2020.106918.

Zhang, L.G., Li, X.Q., Jin, W.T., Liu, Y.J., Zhao, Y., Rong, J., Xiang, X.G., 2023. Asymmetric migration dynamics of the tropical Asian and Australasian floras. Plant Divers. 45, 20–26. https://doi.org/10.1016/j.pld.2022.05.006.

Zhao, H.T., Wang, L.R., Yuan, J.Y., 2007. Origin and time of Qiongzhou Stait. Mar. Geol. Quat. Geol. 27, 33–40. https://doi.org/10.16562/j.cnki.0256 -1492.2007.02.005.

Zhao, C.Y., Xiong, Z.Y., Farnsworth, A., Spicer, R.A., He, S.L., Wang, C., Zeng, D., Cai, F. L., Wang, H.Q., Tain, X.L., Valdes, P.J., Lamu, C., Xie, J., Yue, Y.H., Ding, L., 2023. The rise of SE Tibet formed a late Eocene 'Mediterranean' climate. Glob. Planet. Chang. 231, 104313 https://doi.org/10.1016/j.gloplacha.2023.104313.

Zhu, H., 2016. Biogeographical evidences help revealing the origin of Hainan Island. PLoS One 11, e0151941.

Zhu, H., 2017. Families and genera of seed plants in relation to biogeographical origin on Hainan Island. Biodivers. Sci. 25, 816–822. https://doi.org/10.17520/biods.2017009.

Zhu, H., 2020. On the biogeographical origin of Hainan Island in China. Plant Sci. J. 38, 839–843.